



Cracks fail to intensify stress in nacreous composites

Haimin Yao^{a,b,*}, Zhigong Song^c, Zhiping Xu^c, Huajian Gao^d

^aDepartment of Mechanical Engineering, The Hong Kong Polytechnic University, Hung Hom, Kowloon, Hong Kong Special Administrative Region

^bThe Hong Kong Polytechnic University Shenzhen Research Institute, Shenzhen 518057, China

^cDepartment of Engineering Mechanics, Tsinghua University, Beijing 100084, China

^dSchool of Engineering, Brown University, Providence, RI 02912, USA



ARTICLE INFO

Article history:

Received 11 January 2013

Received in revised form 19 March 2013

Accepted 23 March 2013

Available online 1 April 2013

Keywords:

A. Hybrid composites

B. Mechanical properties

C. Damage tolerance

C. Finite element analysis (FEA)

ABSTRACT

Linear elastic fracture mechanics (LEFM) implies that crack-like flaws would intensify stress in brittle materials with stress intensity scaling up with the square root of the crack size. Therefore, the apparent strength of materials tends to be much smaller than the theoretical value. In this paper, we examine the stress state in nacreous composites and find that in such materials the crack-induced stress intensification and its dependence on crack size can be suppressed greatly. This feature of nacreous composites can be attributed to the unique “brick-and-mortar” (B-and-M) structure and a synergistic match of the mechanical properties between “brick” (e.g. minerals) and “mortar” (e.g. proteins) phases. Our findings not only provide a fundamental insight into the origin of the excellent mechanical properties of nacreous composites such as high strength, high toughness and flaw tolerance, but also will be of great value to the design and synthesis of new structural materials for superior mechanical properties.

© 2013 Elsevier Ltd. All rights reserved.

1. Introduction

Brittle materials such as ceramics exhibit “bulk” strength a few orders of magnitude lower than the theoretical values. Such degradation of strength has been commonly attributed to the inevitable existence of crack-like flaws in the materials. In the presence of cracks, the stress in a material, even under relatively low applied load, can be locally intensified to a level high enough to initiate crack growth, resulting in much reduced apparent strength. In order to design materials with high strength, crack-induced stress intensification is a fundamental issue needs to be tackled. Surprisingly, this intractable problem seems to have been successfully addressed in natural biomaterials whose major compositions are actually brittle minerals. Nacre, for example, is composed of more than 95 vol% of aragonite and less than 5 vol% of proteins [1], but its *apparent tensile strength* reaches up to 300 MPa [2], an order of magnitude higher than that of the pure monolithic aragonite. Such high apparent strength in combination with a high content of brittle constituent implies that there must be certain mechanisms in nacre’s structure and/or material effectively suppressing the crack-induced stress intensification.

It is a common structural feature of load-bearing biological materials such as nacre, teeth and bone that their stiff constituent phases (e.g. minerals) are normally present in the form of thin

tablets or elongated fibers glued together by the soft constituent phases (e.g. proteins), resulting in the so-called “brick-and-mortar” (B-and-M) structure [3], as shown in Fig. 1a. In nacre, the thickness of the bricks is generally much greater than that of the mortar, giving rise to a high volume fraction of the brick phase (the thicknesses of aragonite tablets and protein layer are around 500 nm and 25 nm respectively). Inspired by the natural B-and-M composites, Gao et al. [3,4] showed that the crack-induced stress concentration in an individual brick vanishes when the brick thickness is reduced to below a critical length scale around a few tens of nanometers, reaching the so-called *flaw tolerance* state [5,6]. This concept was also applied to the robust adhesion of nanoscale fibrillar structures [7,8] and observed in nanocrystalline graphene [9]. For nacreous B-and-M materials, nanoscale dimension plays an important role in preventing the crack-induced stress concentration in individual bricks. But what about stress concentration caused by cracks larger than the thickness of individual bricks? Can the nacreous materials tolerate cracks larger than the brick thickness? To answer these questions, further explorations into the stress field in B-and-M materials is needed.

2. Distribution of shear stress in mortar layer

To shed light on the stress field in materials with the B-and-M composite structure, many theoretical attempts have been made based on a variety of assumptions for the structure and constitutive law of the composite. As our attention in this paper is mainly

* Corresponding author at: Department of Mechanical Engineering, The Hong Kong Polytechnic University, Hung Hom, Kowloon, Hong Kong.

E-mail address: mmhyao@polyu.edu.hk (H. Yao).

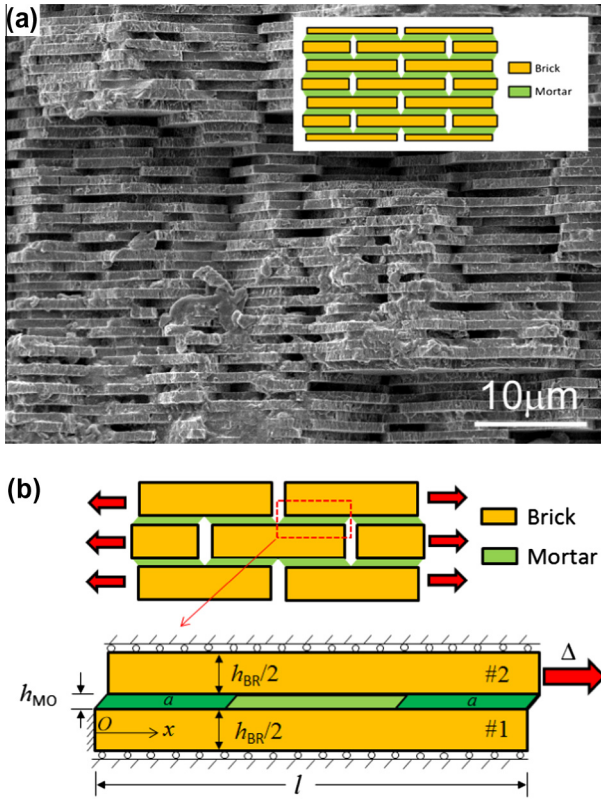


Fig. 1. (a) SEM image of brick-and-mortar structure in nacre; and (b) schematics of a TSC model under uniaxial tension. Due to the periodicity and symmetry of the problem, an assembly of a mortar layer sandwiched by two quarter bricks is used as a representative unit cell for analysis.

focused on the spatial distribution of stresses, we propose a simplified model by referring to recent studies [10–12].

Let us begin with stress in the mortar layer. As has been indicated by the “tension-shear chain” (TSC) model [3,13], the stress in the mortar layer of a B-and-M composite is dominantly shear. The distribution of the shear stress depends on the mechanical properties of brick and mortar as well as the remote external loading. Consider an infinite B-and-M composite under uniaxial tension along the longitudinal direction of bricks, as illustrated in Fig. 1b. The periodicity and symmetry of the B-and-M structure allows us to tackle the problem simply by considering a unit cell consisting of a mortar layer sandwiched by two quarter bricks marked by #1 and #2. Periodic boundary condition is applied by constraining the transverse movements of the lateral boundaries. While the mortar is assumed to be elastic perfectly plastic with shear modulus G_{MO} and shear strength τ_0 , the bricks are modeled as elastic material with Young’s modulus E_{BR} and strength σ_{th}^f . The end-to-end elongation of two bricks under external uniaxial load is denoted by Δ , as shown in Fig. 1b. If Δ is small, the mortar layer undergoes purely elastic deformation and the shear stress therein is correlated with the relative longitudinal displacements between bricks #1 and #2 through

$$\tau(x) = [u_2(x) - u_1(x)] \frac{G_{MO}}{h_{MO}},$$

where \sqrt{a} is the thickness of the mortar layer, and u_1 and u_2 are the longitudinal displacements of bricks #1 and #2, respectively. The symmetry of the problem implies that $u_2(x) = \Delta - u_1(l - x)$, where l is the half length of bricks. As the shear stress developed in the mortar layer is applied on the surface of brick #1 and balanced by the normal stress $\sigma(x)$ in it, we have

$\tau(x) = -\frac{h_{BR}}{2} \frac{d\sigma(x)}{dx} = -\frac{h_{BR}E_{BR}}{2} u_1''(x)$, where h_{BR} is the thickness of the brick. It follows that

$$u_1''(x) = [u_1(l - x) + u_1(x) - \Delta] \frac{2G_{MO}}{h_{BR}h_{MO}E_{BR}}. \quad (1)$$

Such “shear lag” type of approach was originally proposed by Cox [14] and has been widely used in analyzing the stress transfer in composites [15–18]. The solution to the Eq. (1) is readily obtained by adopting proper boundary conditions. The detailed procedure can be found in Appendix A of the Electronic Supplementary Materials (ESM). The distribution of shear stress in the mortar is then given by

$$\tau(x) = \frac{G_{MO}\Delta}{h_{MO}} \left[\frac{\cosh(2\mu x/l - \mu)}{\cosh \mu + \mu \cdot \sinh \mu} \right], \quad (2)$$

where μ is a dimensionless parameter defined as $\mu = \sqrt{\frac{\rho G_{MO}}{h_{BR}h_{MO}E_{BR}}}$. Similar solutions have been obtained in previous studies [10,11,19]. Denoting the aspect ratio of bricks by $\rho = 2l/h_{BR}$, μ can be rewritten as $\mu = \frac{\rho}{2} \sqrt{\frac{h_{BR}G_{MO}}{h_{MO}E_{BR}}} \approx \frac{\rho}{2} \sqrt{\frac{\Phi G_{MO}}{(1-\Phi)E_{BR}}}$, where $\Phi \approx \frac{h_{BR}}{h_{BR}+h_{MO}}$ stands for the volume fraction of the brick phase. It is implied that higher stiffness ratio E_{BR}/G_{MO} between brick and mortar or lower aspect ratio ρ of brick give rise to lower value of μ . For the limiting case of rigid bricks, μ is reduced to 0, giving rise to a uniform distribution of shear stress $\frac{G_{MO}\Delta}{h_{MO}}$ according to Eq. (2). For the other cases with $\mu = 0.5, 1.0, 5.0$ and 10.0 , the distributions of shear stress given in Eq. (2) are graphically shown in Fig. 2a. It can be seen that for given μ the maximum shear stress occurs at the ends $x = 0$ and $x = l$, while the minimum takes place at the middle $x = l/2$. The ratio of the maximum to the minimum can be readily calculated from Eq. (2) and equals $\cosh \mu$, which is actually a monotonically increasing function of μ . For nacre, if we take $E_{BR} = 100$ GPa, $h_{BR} = 500$ nm, $h_{MO} = 25$ nm, $l = 3.75$ μm , $G_{MO} = 33.56$ MPa (based on $E_{MO} = 100$ MPa and

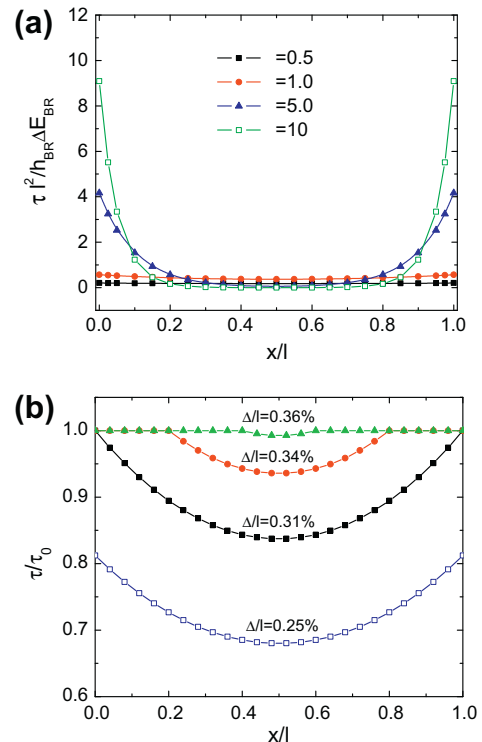


Fig. 2. (a) Distribution of shear stress in mortar layer under elastic deformation. (b) Distribution of shear stress in elastic-perfectly-plastic mortar layer under different levels of external load.

$v_{MO} = 0.49$) (the same values will be adopted throughout this paper unless otherwise indicated), μ is estimated to be around 0.614. The ratio of the maximum to minimum shear stresses is estimated to be around 1.2, implying little variation of shear stress within the mortar layer in nacre. Recalling the definition of μ , it is evident that even more homogeneous shear stress field will be developed if nacreous materials have higher stiffness ratio between brick and mortar E_{BR}/G_{MO} or lower aspect ratio of bricks ρ .

In the preceding analysis, we assumed that the deformation of mortar is purely elastic. This is true only when Δ is smaller than the critical value given by $\Delta_c = l\beta^2[1 + \mu \tanh(\mu)]$, where β is a dimensionless parameter defined as $\beta = \sqrt{\frac{h_{MO}\tau_0}{G_{MO}l}}$. For nacre, taking $h_{MO} = 25$ nm, $\tau_0 = 11.55$ MPa (as Von Mises yield criterion implies that $\tau_0 = \sigma_y/\sqrt{3}$, where σ_y is the tensile yield strength of protein taken as 20 MPa here), $G_{MO} = 33.56$ MPa and $l = 3.75$ μ m leads to an estimate of β to be 0.048. It follows that the critical displacement Δ_c is around 0.31% provided that $\mu = 0.614$ as we estimated before. When the elongation Δ exceeds the critical value Δ_c , plastic yielding in mortar takes place starting from ends $x = 0$ and $x = l$. According to the magnitude of shear stress, the mortar layer can be divided into yielding zones and elastic zone, as shown in Fig. 2b. In the yielding zones ($0 < x < a$ and $1 - a < x < 1$), shear stress is uniform and equal to the shear strength τ_0 . In the elastic zone ($a \leq x \leq l - a$), the longitudinal displacement of brick #1 $u_1(x)$ should satisfy Eq. (1), leading to the following equations:

$$u_1''(x) = \begin{cases} -\frac{2\tau_0}{h_{BR}E_{BR}}, & (0 \leq x \leq a \text{ or } l - a \leq x \leq l) \\ \frac{2C_{MO}}{h_{BR}h_{MO}E_{BR}}[u_1(l - x) + u_1(x) - \Delta], & (a \leq x \leq l - a) \end{cases} \quad (3)$$

The solution to Eq. (3) can be readily obtained by using proper boundary conditions (see Appendix B of the Electronic Supplementary Materials for the details), and the shear stress in mortar is found to be

$$\tau(x) = \begin{cases} \frac{\cosh(2\mu x/l - \mu)}{\cosh(2\mu a/l - \mu)} \tau_0, & (a \leq x \leq l - a) \\ \tau_0, & (x < a \text{ or } x > l - a) \end{cases} \quad (4)$$

with the length of the yielding zone a determined implicitly from the following equation (see Appendix B for detailed derivation):

$$\Delta = 2\beta^2\mu^2a(a/l + 1) + \beta^2l - \beta^2\mu(l + 2a)\tanh(2\mu a/l - \mu). \quad (5)$$

By taking $\mu = 0.614$ and $\beta = 0.048$ for nacre, Fig. 2b shows the distributions of shear stress in the mortar after consideration of yielding. It can be seen that the yielding of mortar initiates at $x = 0$ and $x = l$ when Δ reaches 0.31%. The yielding zone further expands with the increase of Δ . Eventually, when $\Delta \approx 0.36\%l$, the mortar layer yields completely, giving rise to a uniform shear stress equal to τ_0 over the whole mortar layer. It should be pointed out that our analysis is based on the assumption that the mortar and mortar/brick interface would not fail before full yielding. This assumption is reasonable for B-and-M composites with highly deformable mortar such as proteins in nacre. For the case with less ductile mortar, failure of mortar may occur before the whole layer yields. Under this circumstance, more sophisticated modeling is needed, which is beyond the scope of the present paper.

Our analysis so far has indicated that the shear stress in the mortar layer of nacre exhibits little variation at both elastic and plastic stages of deformation. At the purely elastic stage, the shear stress is homogenized due to the exceedingly high stiffness ratio (>1000) between minerals and proteins. With increasing load, such shear stress gets further homogenized as plastic yielding of proteins happens. Eventually, a uniform shear stress is developed in the protein layer (mortar) with magnitude capped by its shear

strength τ_0 . Such shear stress is transferred through the mineral/protein interfaces and imposed on the mineral surfaces as tangential traction, giving rise to tensile stress in the minerals (bricks).

3. Capped stress concentration in bricks

The tensile stress developed in a brick depends on the magnitude and distribution of the tangential traction τ applied on it. What we are interested here is the stress concentration of the tensile stress σ in bricks, which strongly relies on the spatial distribution of the tangential traction τ . To examine the dependence of stress concentration of the normal stress in bricks on the distribution of tangential tractions τ , the plane strain problem of a two-dimensional brick with aspect ratio ρ is considered. The tangential traction, which is a function of dimensionless parameter μ as given in Eq. (2), is applied on both sides of the brick. Finite element analysis (ABAQUS, Dassault Systèmes) is carried out to examine the stress concentration factor of the tensile stress in the brick, which is defined as the ratio of the maximum tensile stress to the mean value over the cross-section. Fig. 3a shows the evolution of stress concentration factor as a function of μ for bricks with different aspect ratios ρ . For a given ρ , it can be seen that the stress concentration factor decreases with decreasing μ , implying that larger discrepancy between mortar and brick in stiffness tends to mitigate stress concentration in the bricks. In the limiting case of $\mu = 0$, corresponding to uniform tangential traction, the stress concentration factor drops to a value close to unity for the aspect ratio of $\rho = 32$. Such trend was also confirmed by molecular dynamic (MD) simulations (see Appendix C of the Electronic Supplementary Materials for details). For nacre, if we take $\rho = 15$ and $\mu = 0.614$, it can be estimated from Fig. 3a that the stress concentration factor is around 1.4. Since $\mu = \frac{\rho}{2} \sqrt{\frac{\Phi G_{MO}}{(1-\Phi)E_{BR}}}$, the stress concentration factor can also be expressed in terms of two independent variables $\sqrt{\frac{\Phi G_{MO}}{(1-\Phi)E_{BR}}}$ and ρ , as shown in Fig. 3b. It can be clearly seen that higher aspect ratio of brick or larger stiffness difference between brick and

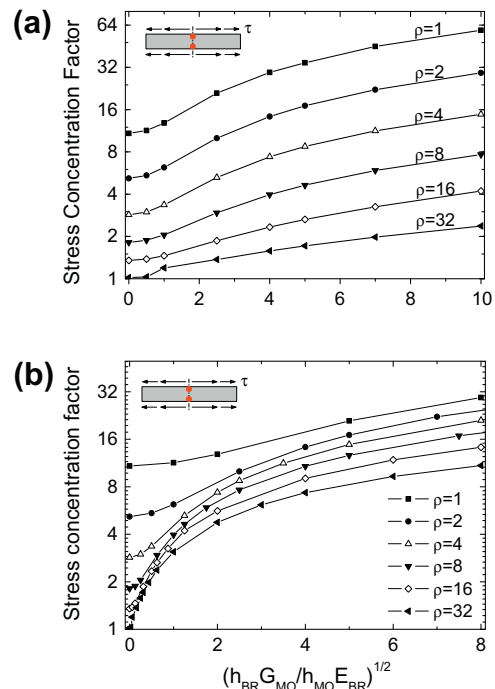


Fig. 3. (a) Variation of stress concentration factor with μ for different aspect ratio ρ ; and (b) variations of stress concentration factor with $\sqrt{\frac{h_{BR} G_{MO}}{h_{MO} E_{BR}}}$ for different ρ .

mortar would result in less stress concentration in bricks. For nacre, the volume fraction Φ is as high as 95%. The stiffness of brick is about three orders of magnitude greater than that of the mortar, giving rise to the ratio of G_{MO}/E_{BR} approximately equal to 10^{-3} . It is this small stiffness ratio in combination with the large aspect ratio of brick ensures the capped stress concentration in nacre. Similar reduction of stress concentration due to the large stiffness difference between protein and mineral has been reported by Okumura and de Gennes [20], even though the effect of aspect ratio of brick on stress concentration was not considered in their work.

Although the yielding of mortar has not been taken into account in Fig. 3, it can be predicted that the stress concentration factor will become even smaller if the mortar starts to yield as the shear stress in mortar layer becomes more homogeneous. If full yielding is achieved in the mortar layer, the tangential traction applied on the brick surfaces would become uniform and equal to the shear strength τ_0 of mortar. The tensile stress in brick then exhibits the same extent of stress concentration as that in the elastic case with $\mu = 0$. Therefore, the maximum tensile stress in nacre is always less than 1.4 times the mean tension over the cross-section, which should not exceed $\tau_0\rho$ with τ_0, ρ being the shear strength of the mortar and aspect ratio of the brick, respectively. If the tensile fracture strength of bricks $\sigma_{th}^f \geq 1.4\tau_0\rho$ or $E_{BR} \geq 42\tau_0\rho$ taking $\sigma_{th}^f \approx E_{BR}/30$, the bricks would never fracture. The validity of above condition can be easily verified if we choose $\tau_0 \approx 11.55$ MPa, $E_{BR} = 50$ GPa and $\rho \approx 15$ for nacre. If we consider the interfacial strengthening mechanisms in real nacre such as “intertile bridges” and asperities by taking τ_0 as the value of interfacial shear strength, which was measured to be around 37 MPa [21], above condition is still satisfied.

So far, our discussion on the stress concentration in bricks is carried out by using the perfect intact B-and-M model. In reality,

however, not all bricks in nacre are strong. Some weak bricks may exist due to the existence of preexisting cracks. Under external loading, fracture happens first in the weakest bricks, resulting in cracks larger than the thickness of individual brick. Will these larger cracks cause higher stress concentration as in monolithic brittle materials and eventually lead to catastrophic failure? To answer this question, a cracked B-and-M model is constructed by introducing a few broken bricks in advance, as shown in Fig. 4a. The size of the crack is given by $2a = (2n + 1)h_{BR} + (2n + 2)h_{MO}$, where n is the number of the broken bricks introduced. The bricks and mortar are assumed as elastic and elastic-perfectly-plastic materials respectively, with mechanical properties taken as those adopted above. Uniaxial tension is applied along the longitudinal direction with periodic boundary conditions applied on both sides of the model. Therefore, what we are considering here is actually a nacreous material with periodic crack configuration. The width of model W represents the spatial periodicity, which is taken as $12.6 \mu\text{m}$ in our model. Finite element analysis (ABAQUS, Dassault Systèmes, France) is adopted to examine the maximum tensile stress in the bricks.

For different crack sizes $2a$, Fig. 4b displays the calculated distributions of the tensile stress at the moment when the maximum tensile stress in bricks occurs. Clearly, stress concentration of certain extent is present in the bricks located in the vicinity of the crack tips. The variation of the maximum tensile stress with the crack size is shown in Fig. 4c. It can be seen that the maximum tensile stress in the bricks firstly increases and then decreases with the increase of crack size. Like the prediction by the intact B-and-M model above, our calculation on the basis of the cracked nacre model indicates that the maximum tensile stress in bricks is still capped by a finite value irrespective of the crack size $2a$. In the calculated case, this finite value is less than $1.45\rho\tau_0$. That is, the

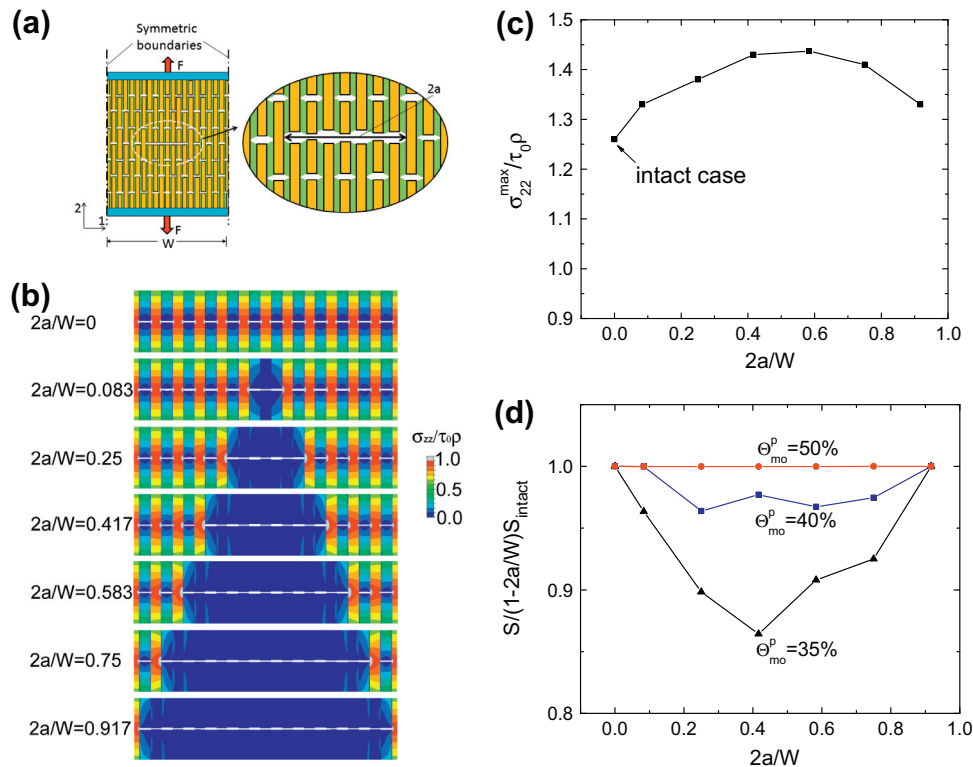


Fig. 4. (a) Schematics of cracked B-and-M structured materials under uniaxial tension. (b) Close-ups of the tensile stress in cracked B-and-M composites with cracks of various sizes. (c) Variation of the normalized maximum tensile stress in cracked B-and-M composites as a function of normalized crack size. (d) Calculated variation of normalized effective tensile strength of cracked nacreous materials as a function of crack size with the failure shear strain of mortar layer being taken as 35%, 40% and 50% respectively.

crack-induced stress intensification is always limited within a finite level in nacreous materials regardless of the crack size. Therefore, the bricks in nacreous materials would not fracture as long as their theoretical strength σ_{th}^f is no less than a finite threshold $k\tau_0\rho$, where k is a constant depending on the aspect ratio ρ of bricks and stiffness ratio between brick and mortar. In our calculated case, $k=1.45$. Clearly, such capped stress concentration would never be expected in monolithic materials with dimension more than microns, in which crack with the configuration shown in Fig. 4a would result in stress intensity proportional to $\sqrt{W \cdot \tan(\pi a/W)}$ [22], a quantity growing monotonically as $2a/W$ approaches to unity. To shed light on the load-bearing capacity of cracked nacreous composites, the *effective tensile strength* (ETS) is examined, which is defined as the maximum sustainable tensile force per unit effective bonded area on the plane of crack, i.e. $S = F_{max}/(W - 2a)$. Fig. 4d shows the calculated ETS of the cracked nacreous materials as a function of crack size. Mortar layer with different failure shear strain θ_{MO}^p or ductility are considered. Our results show that the variation of the ETS with the crack size depends on the ductility of mortar. When $\theta_{MO}^p = 35\%$, ETS exhibits apparent degradation in comparison to the strength of the intact case ($a=0$). Such degradation is reduced with the increase of θ_{MO}^p . There exists a critical value of θ_{MO}^p beyond which the ETS of the cracked nacreous materials is constant and equal to the strength of the intact case S_{intact} irrespective of the crack size, implying that the *flaw tolerance* state is achieved within the size of W . In our computational model W is taken as $12.6 \mu\text{m}$ and the critical θ_{MO}^p for flaw tolerance is around 50%. To achieve flaw tolerance at even larger length scale, mortar with higher ductility or larger θ_{MO}^p is required. This is basically due to the dependence of length scale for flaw tolerance on the fracture energy [6] which, for nacreous composites, is proportional to the ductility of mortar layer θ_{MO}^p .

4. Conclusions and discussion

Crack-like flaws have long been viewed as destructive elements for structural materials as they tend to intensify stress with intensity factor scaling up with the crack size. Theoretically, the intensified stress at the tip of a crack can reach any level required to break the microscopic bonds of the material, leading to the growth of crack. The growth of crack size in return will degrade the carrying capacity of the material further, resulting in catastrophic failure and lower apparent strength. In this paper, exploration into the stress state of B-and-M composites indicated that such crack-induced stress intensification can be suppressed in B-and-M structured materials. That is because in B-and-M materials the load is transferred through brick/mortar interfaces. If the mortar phase is compliant and ductile, the load applied on the bricks is always confined by the shear strength of mortar. The maximum tensile stress developed in the bricks is capped by a finite value independent of the crack size. Catastrophic failure of material is effectively avoided and considerable strength of the composite is ensured. Besides, the capped stress state in the bricks also benefits the toughness of the B-and-M composite because it prevents the cracks from propagating into bricks. Therefore, the cracks would deflect when encountering the brick/mortar interfaces [23]. As a consequence, delamination of brick/mortar interface or fracture of mortar occurs, triggering a variety of toughening mechanisms including pullout of the bricks from the mortar matrix, interfacial friction, sliding of bricks and so on [24,25].

It should be pointed out that capped stress concentration is not a ubiquitous nature of all B-and-M composites. Instead, the occurring of it is conditional and dependent on factors such as the stiffness ratio between brick and mortar phases, the aspect ratio of the

bricks and the volume fraction of bricks. While higher volume fraction of brick phase would make the stress in the mortar layer shear-dominant, the higher stiffness ratio between brick and mortar and larger aspect ratio of bricks would homogenize the distribution of the shear stress in the mortar layer. Additionally, the theoretical strength of bricks σ_{th}^f should be no less than $k\rho\tau_0$, where k is a coefficient. For B-and-M structure with large aspect ratio of brick and high stiffness ratio between brick and mortar, k approaches 1. For nacre, it can be readily verified that all above conditions are satisfied very well, giving rise to its excellent mechanical properties. These findings not only shed light on the origin of the high strength, high toughness and flaw tolerance of natural nacreous materials, but also would be of great value to the design and fabrication of biomimetic nacreous materials.

Acknowledgements

Partial supports for this work from the Departmental General Research Funds (A-PM24, 4-ZZA8 & G-UA20) of the Hong Kong Polytechnic University and Natural Science Foundation of China (Grant No. 11072273) are acknowledged. HY would like to thank Prof. Yong Ni from University of Science and Technology of China for the stimulating discussions on biomaterials. HG gratefully acknowledges support from the University of Hong Kong through the Distinguished Visiting Scholars Scheme (DVSS).

Appendix A. Supplementary material

Supplementary data associated with this article can be found, in the online version, at <http://dx.doi.org/10.1016/j.compscitech.2013.03.016>.

References

- [1] Meyers MA, Chen PY, Lin A, Seki Y. Biological materials: structure and mechanical properties. *Prog Mater Sci* 2008;53:1–206.
- [2] Jackson AP, Vincent JFV, Turner RM. The mechanical design of nacre. *Proc Royal Soc London Series B – Biol Sci* 1988;234(1277):415–40.
- [3] Gao HJ, Ji BH, Jager IL, Arzt E, Fratzl P. Materials become insensitive to flaws at nanoscale: lessons from nature. *Proc Natl Acad Sci USA* 2003;100(10):5597–600.
- [4] Ji B, Gao H. Mechanical properties of nanostructure of biological materials. *J Mech Phys Solids* 2004;52(9):1963–90.
- [5] Gao H, Ji B, Buehler MJ, Yao H. Flaw tolerant nanostructures of biological materials. In: Gutkowsky W, Kowalewski TA, editors. *Mechanics of the 21st century*. Dordrecht (Netherlands): Springer; 2005.
- [6] Gao H, Chen S. Flaw tolerance in a thin strip under tension. *J Appl Mech* 2005;72:732–7.
- [7] Gao H, Yao H. Shape insensitive optimal adhesion of nanoscale fibrillar structures. *Proc Natl Acad Sci USA* 2004;101:7851–6.
- [8] Yao H, Gao H. Mechanics of robust and releasable adhesion in biology: bottom-up designed hierarchical structures of gecko. *J Mech Phys Solids* 2006;54:1120–46.
- [9] Zhang T, Li X, Kadkhodaei S, Gao H. Flaw insensitive fracture in nanocrystalline graphene. *Nano Lett* 2012;12:4605–10.
- [10] Liu G, Ji B, Hwang KC, Khoo BC. Analytical solutions of the displacement and stress fields of the nanocomposite structure of biological materials. *Compos Sci Technol* 2011;71:1190–5.
- [11] Bar-on B, Wagner HD. Mechanical model for staggered bio-structure. *J Mech Phys Solid* 2011;59:1701–965.
- [12] Bar-on B, Wagner HD. Elastic modulus of hard tissues. *J Biomech* 2012;45:672–8.
- [13] Jäger I, Fratzl P. Mineralized collagen fibrils: a mechanical model with a staggered arrangement of mineral particles. *Biophys J* 2000;79:1737–46.
- [14] Cox HL. The elasticity and strength of paper and other fibrous materials. *Br J Appl Phys* 1952;3:72–9.
- [15] Kim JK, Baillie C, Mai YM. Interfacial debonding and fibre pull-out stresses. Part I: critical comparison of existing theories. *J Mater Sci* 1992;27:3143–54.
- [16] Begley MR, Philips NR, Compton BG, Wilbrink DV, Ritchie RO, Utz M. Micromechanical models to guide the development of synthetic ‘brick and mortar’ composites. *J Mech Phys Solid* 2012;60:1545–60.
- [17] Jiang KR, Penn LS. Improved analysis and experimental evaluation of the single filament pull-out test. *Compos Sci Technol* 1992;45:89–103.
- [18] Nairn JA. On the use of shear-lag methods for analysis of stress transfer in unidirectional composites. *Mech Mater* 1997;26:63–80.

- [19] Chen B, Wu PD, Gao H. A characteristic length for stress transfer in the nanostructure of biological composites. *Compos Sci Technol* 2009;69:1160–4.
- [20] Okumura K, de Gennes P-G. Why is nacre strong? Elastic theory and fracture mechanics for biocomposites with stratified structures. *Eur Phys J E* 2001;4:121–7.
- [21] Lin Y-M, Meyers MA. Interfacial shear strength in abalone nacre. *J Mech Behav Biomed Mater* 2009;2(6):607–12.
- [22] Anderson TL. *Fracture mechanics: fundamentals and applications*. 3rd ed. New York: CRC Press; 2005.
- [23] Parmigiani J, Thouless M. The roles of toughness and cohesive strength on crack deflection at interfaces. *J Mech Phys Solid* 2006;54(2):266–87.
- [24] Sarikaya M, Liu J, Aksay IA. Nacre: properties, crystallography, morphology and formation. In: Sarikaya M, Aksay IA, editors. *Biomimetics: design and processing of materials*. American Institute of Physics; 1995. p. 35–90.
- [25] Sarikaya M, Gunnison KE, Yasrebi M, Aksay JA. Mechanical property – microstructural relationships in abalone shell. *Mater Res Soc Symp Proc* 1990;174:109–16.